

THE $e^+e^- \rightarrow Z\phi \rightarrow l^-l^+b\bar{b}$ COLLISION IN THE RANDALL-SUNDRUM MODEL**Bui Thi Ha Giang***Faculty of Physics, Hanoi National University of Education*

Abstract. Taking account of the Randall-Sundrum model, we have evaluated the influence of model parameters in $e^+e^- \rightarrow Z\phi \rightarrow l^-l^+b\bar{b}$ collision at International Linear Colliders (ILC). In the ILC region, the total cross-section is enhanced at the 125 GeV radion. The total cross-section depends on the polarization of e^- , e^+ initial beams, the radion mass m_ϕ , the center of mass energy \sqrt{s} . Based on the forward - backward asymmetry and the polarization of beams, the reaction can give observable cross-sections based on $l^-l^+b\bar{b}$ final state.

Keywords: Randall-Sundrum model, radion mass, cross-section, anomalous couplings.

1. Introduction

The Randall-Sundrum (RS) model, one of some models beyond the Standard Model (SM), has been aimed at solving the hierarchy problem [1]. The RS model with IR and UV three-branes has allowed the appearance of an additional scalar called the radion (ϕ), which has been expected to be the lightest new gravity state [2]. Based on the same quantum numbers, radion and Higgs boson can be mixed [3-7].

Due to the light radion with a mass below 100 GeV, the Z resonance peak can be detected at the ILC. The radion mass eigenstate contains a heavy mixture of the SM Higgs boson when its mass is near $m_h = 125$ GeV [8]. The parameter value region which is difficult to detect at Large Hadron Colliders (LHC) could be examined by the associated production of Z boson and the heavy radion with the $b\bar{b}$ final state. This channel is better suited to analyze at ILC [6]. The radion couplings to $Z\gamma$ is dominated in the region $\xi[0,0.3]$ [9]. It is interested in the radion couplings in the conformal limit $\xi=1/6$. Moreover, linear colliders with the electron and positron beams have the cleaner backgrounds and signals. Therefore, the ILC is an ideal laboratory to study new physics. In this work, we also choose electron and positron beams as the initial beams at ILC with the energy from 500 GeV – 1 TeV [10].

Received August 4, 2021. Revised October 15, 2021. Accepted October 22, 2021.

Contact Bui Thi Ha Giang, e-mail address: giangbth@hnue.edu.vn

In this work, we analyze the $Z\phi$ associated production, followed by Z boson decaying leptonically, the radion decay into $b\bar{b}$. The main motivation of this study is to show the influence of the polarization coefficients of e^-, e^+ beams in exploring the $l^+l^-\bar{b}b$ scenario at the ILC.

2. Content

In our previous work [11], the anomalous couplings of the radion to $Z\gamma$ was neglected. Therefore, in the present study, we have assessed the total cross-section in e^-e^+ scattering, included $\phi Z\gamma, \phi ZZ, \phi\gamma\gamma$ vertices which are not in the SM. Due to the maximum cross-section value at the 110 GeV radion [12], we have chosen the radion mass of 110 GeV.

We denote the collision process in which the initial state includes electron (e^-) and positron (e^+), the final state contains the associated production of the heavy radion and Z boson as

$$e^-(p_1) + e^+(p_2) \rightarrow Z(k_1) + \phi(k_2). \quad (1)$$

Let's denote the four momenta p_i, k_i ($i = 1, 2$) of e^-, e^+, Z, ϕ , respectively. Three Feynman diagrams contributing to reaction (1) represent the s, u, t-channels exchange as in Figure 1.

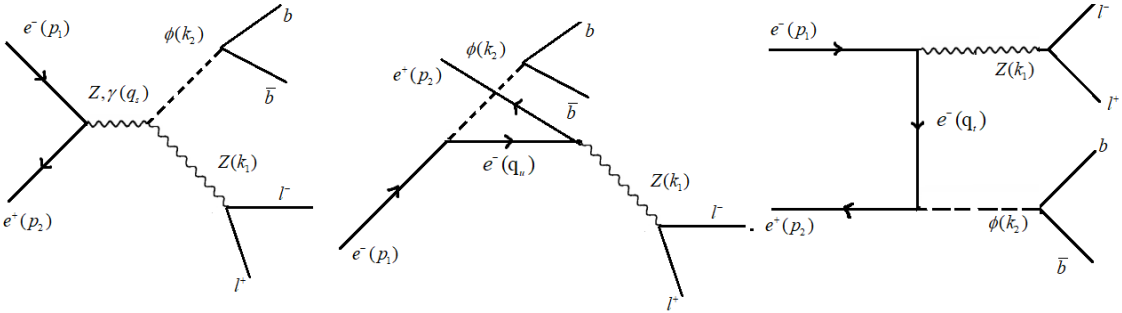


Figure 1. Feynman diagrams of $e^+e^- \rightarrow Z\phi \rightarrow l^+l^-\bar{b}b$ collision in the s, u, t-channels

The transition amplitude corresponding to the s-channel can be obtained as

$$M_s = M_Z + M_\gamma, \quad (2)$$

where

$$M_Z = \frac{-\bar{g}_{\phi Z}}{q_s^2 - m_Z^2} \bar{v}(p_2) \gamma^\mu (v_e - a_e \gamma^5) u(p_1) \left(\eta_{\mu\beta} - \frac{q_{s\mu} q_{s\beta}}{m_Z^2} \right) \left[\eta^{\beta\nu} - 2g_\phi^Z (\eta^{\beta\nu} k_1 q_s - q_s^\nu k_1^\beta) \right] \varepsilon_\nu^*(k_1), \quad (3)$$

$$M_\gamma = \frac{-C_{\gamma Z\phi}}{q_s^2} \bar{v}(p_2) \gamma^\mu (v_e - a_e \gamma^5) u(p_1) \eta_{\mu\beta} \left[\eta^{\beta\nu} k_1 q_s - q_s^\nu k_1^\beta \right] \varepsilon_\nu^*(k_1), \quad (4)$$

The transition amplitude representing the u-channel can be written as

The $e^+e^- \rightarrow Z\phi \rightarrow l^-l^+b\bar{b}$ collision in the Randall-Sundrum model

$$M_u = -i \frac{\bar{g}_{eZ} \bar{g}_{ee\phi}}{q_u^2 - m_e^2} \bar{v}(p_2) (\hat{q}_u + m_e) \varepsilon_v^*(k_1) \gamma^\nu (v_e - a_e \gamma^5) u(p_1). \quad (5)$$

The transition amplitude representing the t-channel is given by

$$M_t = -i \frac{\bar{g}_{eZ} \bar{g}_{ee\phi}}{q_t^2 - m_e^2} \bar{v}(p_2) \gamma^\nu (v_e - a_e \gamma^5) (\hat{q}_t + m_e) \varepsilon_v^*(k_1) u(p_1). \quad (6)$$

where

$$\bar{g}_{\phi Z} = g \frac{m_Z}{\cos \theta_W} (g_\phi - g_\phi^r \kappa_Z), \quad (7)$$

$$C_{\gamma Z\phi} = \frac{\alpha}{2\pi v_0} \left[2g_\phi^r \left(\frac{b_2}{\tan \theta_W} - b_Y \tan \theta_W \right) - g_\phi (A_F + A_W) \right], \quad (8)$$

$$\bar{g}_{ee\phi} = \frac{g m_e}{2m_W} g_\phi. \quad (9)$$

here, $g_\phi, g_\phi^r, \kappa_Z$ can be found in [9, 13-14].

The total cross-section for the whole process $e^+e^- \rightarrow Z\phi \rightarrow l^-l^+b\bar{b}$ can be calculated as follows:

$$\sigma_{total} = \sigma(e^-e^+ \rightarrow Z\phi) \times Br(Z \rightarrow l^+l^-) \times Br(\phi \rightarrow b\bar{b}). \quad (10)$$

where

$$\frac{d\sigma(e^-e^+ \rightarrow Z\phi)}{d(\cos\psi)} = \frac{1}{32\pi s} \frac{|\vec{k}_1|}{|\vec{p}_1|} |M_f|^2 \quad (11)$$

is the expressions of the differential cross-section [15], $\psi = (\vec{p}_1, \vec{k}_1)$ is the scattering angle.

For numerical calculations, we choose ILC running at a center-of-mass energy of 500 GeV and integrated luminosity $\mathcal{L} = 100 fb^{-1}$ [15]. The vacuum expectation value (VEV) of the radion field A_ϕ is 10 TeV [8]. We give estimates for the cross-sections as follows:

(i) In Figure 2, the total cross-section is evaluated to depend on P_{e^-}, P_{e^+} , the polarization coefficients of e^-, e^+ initial beams. The radion mass has been selected $m_\phi = 110$ GeV [6, 12]. The collision energy is taken as $\sqrt{s} = 500$ GeV (ILC). Figure 2 shows that the maximum cross-section value σ_{total} can be as $P_{e^-} = P_{e^+} = \pm 1$ and the minimum cross-section value σ_{total} can be as $P_{e^-} = 1, P_{e^+} = -1$ or $P_{e^-} = -1, P_{e^+} = 1$.

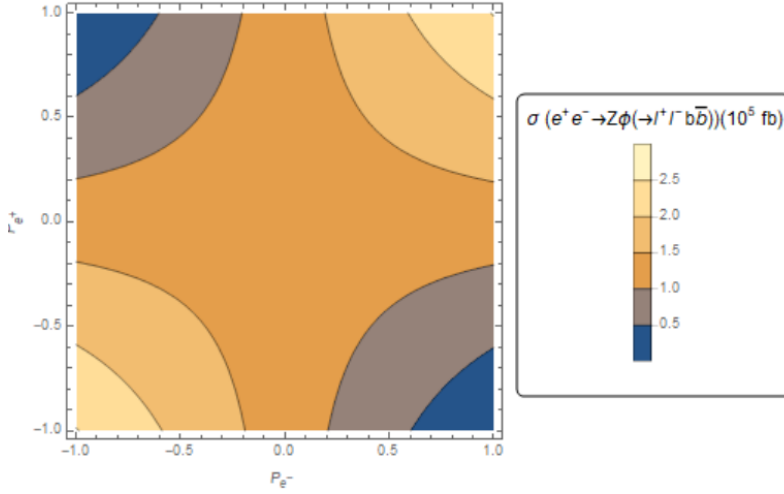


Figure 2. The total cross-section with respect to the polarization coefficients (P_{e^-}, P_{e^+}) in $e^+e^- \rightarrow Z\phi \rightarrow l^+l^-b\bar{b}$ collision at the collision energy of 500 GeV

(ii) The differential cross-sections with respect to $\cos\psi$ can be seen in Figure 3. With the case of $P_{e^-}=0.8, P_{e^+}=-0.3$ [16, 17], in our numerical estimation for $e^+e^- \rightarrow Z\phi \rightarrow l^+l^-b\bar{b}$, the measured forward-backward asymmetry is larger than zero. Moreover, the forward-backward asymmetry increases when the collision energy increases in Figure 4. This result shows the collision energy region and direction to collect the final state from the experiment.

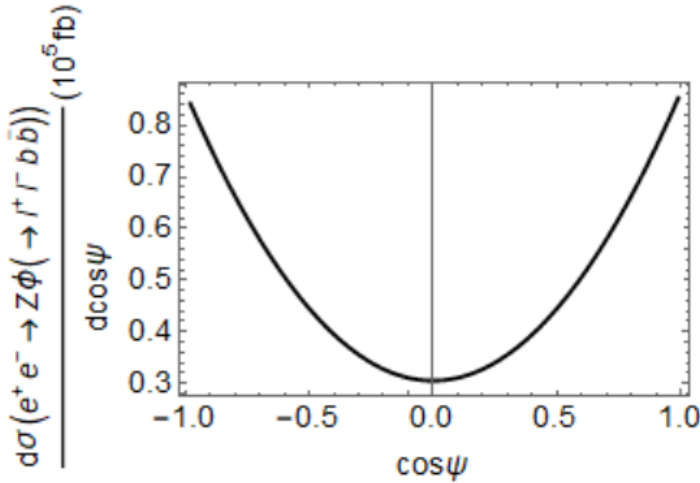


Figure 3. The differential cross-section for the $e^+e^- \rightarrow Z\phi \rightarrow l^+l^-b\bar{b}$ collision as a function of the $\cos\psi$. The model parameters are chosen as $P_{e^-} = 0.8, P_{e^+} = -0.3, \sqrt{s} = 500 \text{ GeV}$

The $e^+e^- \rightarrow Z\phi \rightarrow l^+l^-b\bar{b}$ collision in the Randall-Sundrum model

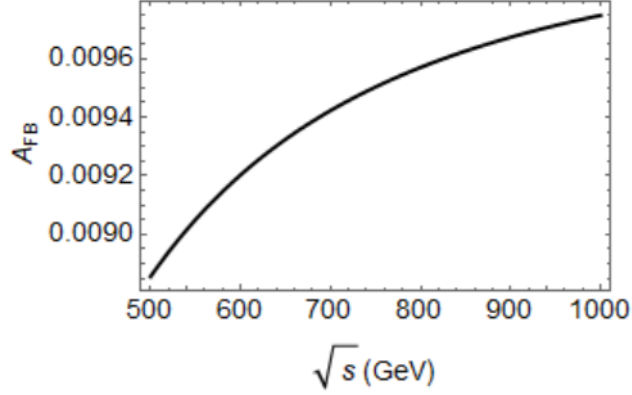


Figure 4. The forward-backward asymmetry with respect to the collision energy \sqrt{s} in $e^+e^- \rightarrow Z\phi \rightarrow l^+l^-b\bar{b}$ collision at $P_{e^-} = 0.8, P_{e^+} = -0.3$

(iii) The collision energy is taken as $\sqrt{s} = 500$ GeV (ILC). In Figure 5, in the radion mass range $100\text{GeV} \leq m_\phi \leq 1\text{TeV}$, the total cross-section starts to climb, reaches a maximum value for the 125 GeV radion, and then falls again rapidly.

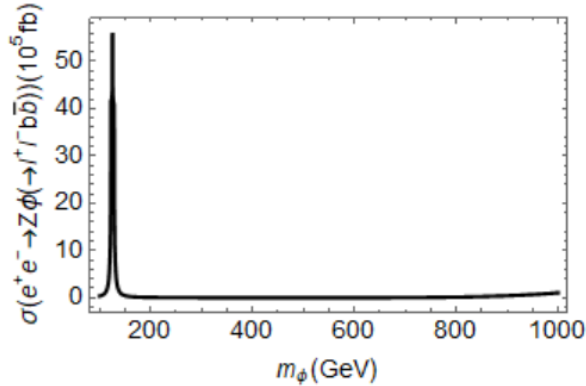


Figure 5. The total cross-section is a function of the radion mass in $e^+e^- \rightarrow Z\phi \rightarrow l^+l^-b\bar{b}$ collision. The polarization coefficients are taken to be $P_{e^-} = 0.8, P_{e^+} = -0.3$

(iv) The polarization coefficients of the initial beams are the same as in Figure 3. The total cross-sections are measured in the case of the various collision energies in Figure 6. This result shows that the total cross-section reduces gradually when the collision energy increases. Some numerical total cross-section values are given in Table 1. With the photon and Z boson contribution in s-channel propagators, the total cross-section is much larger than that only with Z boson contribution in s-channel.

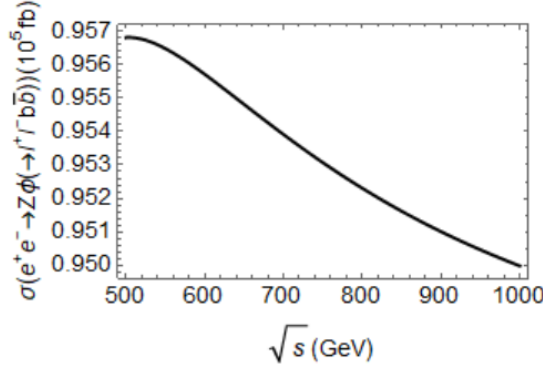


Figure 6. The total cross-section is a function of the energy collision in $e^+e^- \rightarrow Z\phi \rightarrow l^+l^-b\bar{b}$ collision. The polarized e^-, e^+ beams are fixed to $P_{e^-} = 0.8, P_{e^+} = -0.3$

Table 1. The numerical cross-section values in the whole $e^+e^- \rightarrow Z\phi \rightarrow l^+l^-b\bar{b}$ process at different collision energies with $P_{e^-} = 0.8, P_{e^+} = -0.3$ case

The radion mass is taken as 110 GeV

| \sqrt{s} (GeV) | 500 | 600 | 700 | 800 | 900 | 1000 |
|-------------------------------|--------|--------|--------|--------|--------|--------|
| σ_{total} (10^5 fb) | 0.9568 | 0.9557 | 0.9539 | 0.9523 | 0.9510 | 0.9499 |
| σ_Z (fb) | 0.0155 | 0.0246 | 0.0354 | 0.0479 | 0.0620 | 0.0779 |

(v) The curve of the total cross-section in Figure 7 is plotted with respect to the VEV of the radion field Λ_ϕ . In the case of $P_{e^-} = 0.8, P_{e^+} = -0.3$ [16, 17], $\sqrt{s} = 500$ GeV, the total cross-section decreases rapidly in the region $1\text{TeV} \leq \Lambda_\phi \leq 2\text{TeV}$, then gradually in the region $2\text{TeV} \leq \Lambda_\phi \leq 10\text{TeV}$.

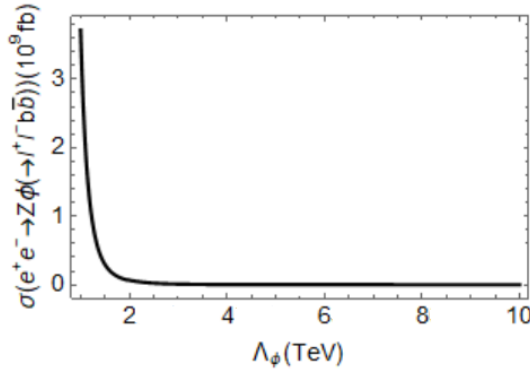


Figure 7. The total cross-section is a function of the VEV of radion field in $e^+e^- \rightarrow Z\phi \rightarrow l^+l^-b\bar{b}$ collision. The polarization of initial beams are taken as $P_{e^-} = 0.8, P_{e^+} = -0.3$

3. Conclusions

In this paper, we have investigated the contribution of the model parameters on the $Z\phi \rightarrow l^+l^-b\bar{b}$ production from e^-e^+ scattering at ILC. The total cross-section reaches the maximum value when both e^- and e^+ beams have been right (left) polarized. With the available value of model parameters $\sqrt{s}, m_\phi, \mathcal{A}_\phi$, the total cross-section can be recorded in the experiment. Due to the $\phi Z\gamma$ anomalous coupling, the total cross-section for $e^+e^- \rightarrow Z\phi \rightarrow l^+l^-b\bar{b}$ scattering is enhanced and much larger than that only with Z propagator in s-channel under the same conditions. The total cross-section of the mixed-radiation state is much larger than that of the unmixed-radiation in Ref. [6].

Acknowledgements: The work is supported in part by the Hanoi National University of Education under Grant No. SPHN21-07.

REFERENCES

- [1] L. Randall and R. Sundrum, 1999. A large mass hierarchy from a small extra dimension, *Phys. Rev. Lett.*, 83, 3370.
- [2] B. M. Dillon, D. P. George and K. L. McDonald, 2016. Regarding the radion in Randall-Sundrum models with brane curvature, *Phys. Rev. D*, 94, 064045.
- [3] C. Csaki, J. Hubisz and S. J. Lee, 2007. Radion phenomenology in realistic warped space models, *Phys. Rev. D*, 76, 125015.
- [4] D. W. Jung, P. Ko, 2014. Higgs-dilaton (radion) system confronting the LHC Higgs data, *Phys. Lett. B*, 732, 364.
- [5] E. Boos, S. Keizerov, E. Rakhmetov, K. Svirina, 2014. Higgs boson radion similarity in production processes involving off-shell fermions, *Phys. Rev. D*, 90, 095026.
- [6] M. Frank, K. Huitu, U. Maitra, M. Patra, 2016. Probing Higgs radion mixing in warped models through complementary searches at the LHC and the ILC, *Phys. Rev. D*, 94, 055016.
- [7] S. A. Li, C. S. Li, H. T. Li, J. Gao, 2015. Constraints on Randall-Sundrum model from the events of dijet production with QCD next to-leading order accuracy at the LHC, *Phys. Rev. D* 91, 014027.
- [8] G. F. Giudice, R. Rattazzi, J. D. Wells, 2001. Gravitational scalars from higher-dimensional metrics and curvature-Higgs mixing, *Nucl. Phys. B*, 595, 250.
- [9] A. Ahmed, B. M. Dillon, B. Grzadkowski, J. F. Gunion and Y. Jiang, 2017. Implications of the absence of high-mass radion signals, *Phys. Rev. D*, 95, 095019.
- [10] H. Yamamoto, 2021. The International Linear Collider Project - Its Physics and Status, *Symmetry*, 13, 674.
- [11] D. T. L. Thuy and B. T. H. Giang, 2016. $e^+e^- \rightarrow hZ$ collision in Randall-Sundrum model, *Comm in Phys*, Vol. 26, No. 1, 19.
- [12] D. V. Soa, D. T. L. Thuy, B. T. H. Giang, 2017. The signal of Higgs from the dominated state 125 GeV in Randall Sundrum model via γe^- colliders, *Adv. Stud. Theor. Phys*, Vol. 11, No. 12, 629.

- [13] D. Dominici, B. Grzadkowski, J. F. Gunion, and M. Toharia, 2003. The scalar sector of the Randall-Sundrum model, *Nucl. Phys. B*, 671, 243.
- [14] B. Grzadkowski, J. F. Gunion, and M. Toharia, 2012. *Phys. Lett. B*, 712, 70.
- [15] M. E. Peskin and D. V. Schroeder, 1995. *An Introduction to Quantum Field Theory*, Addison-Wesley Publishing.
- [16] B. Ananthanarayan, J. Lahiri, M. Patra, and S. D. Rindani, 2014. New physics in $e^+e^- \rightarrow Z\gamma$ at the ILC with polarized beams: explorations beyond conventional anomalous triple gauge boson couplings, *JHEP* 08, 124.
- [17] A. Vauth, J. List, 2016. Beam polarization at the ILC: Physics case and realization, *Int. J. Mod. Phys. Conf. Ser.* 40, 1660003.
- [18] H. Abramowicz *et al.*, 2017. Higgs physics at the CLIC electron positron linear collider, *Eur. Phys. J. C* 77, 475.